



# In situ particle size distributions and volume concentrations from a LISST-100 laser particle sizer and a digital floc camera

Ole A. Mikkelsen<sup>a,b,\*</sup>, Paul S. Hill<sup>a</sup>, Timothy G. Milligan<sup>b</sup>, Robert J. Chant<sup>c</sup>

<sup>a</sup>*Department of Oceanography, Dalhousie University, 1355 Oxford Street, Halifax Nova Scotia, Canada B3H 4J1*

<sup>b</sup>*Department of Fisheries and Oceans, Bedford Institute of Oceanography, PO Box 1006, Dartmouth Nova Scotia, Canada B2Y 4A2*

<sup>c</sup>*Institute of Marine and Coastal Sciences, Rutgers University, 71 Dudley Road New Brunswick, NJ 08901, USA*

Received 21 July 2004; received in revised form 28 June 2005; accepted 4 July 2005

Available online 22 August 2005

## Abstract

A LISST-100 in situ laser particle sizer was deployed together with a digital floc camera during field work in the Newark Bay area (USA) and along the Apennine margin (the Adriatic Sea, Italy). The purpose of these simultaneous deployments was to investigate how well in situ particle (floc) sizes and volume concentrations from the two different instruments compared. In the Adriatic Sea the two instruments displayed the same temporal variation, but the LISST provided lower estimates of floc size by a factor of 2–3, compared to the DFC. In the Newark Bay area, the LISST provided higher values of floc size by up to a factor of 2. When floc size was computed using only the overlapping size bins from the two instruments the discrepancy disappeared. The reason for the discrepancy in size was found to be related to several issues: First, the LISST measured particles in the 2.5–500  $\mu\text{m}$  range, whereas the camera measured particles in the 135–9900  $\mu\text{m}$  range, so generally the LISST should provide lower estimates of floc size, as it measures the smaller particles. Second, in the Newark Bay area scattering from particles  $> 500 \mu\text{m}$  generally caused the LISST to overestimate the volume of particles in its largest size bin, thereby increasing apparent floc size. Relative to the camera, the LISST generally provided estimates of total floc volume that were lower by a factor of 3. Factors that could explain this discrepancy are errors arising from the accuracy of the LISST volume conversion coefficient and image processing. Regardless of these discrepancies, the shapes of the size spectra from the instruments were similar in the regions of overlap and could be matched by multiplying with an appropriate correction coefficient. This facilitated merging of the size spectra from the LISST and the DFC, yielding size spectra in the 2.5–9900  $\mu\text{m}$  range. The merged size spectra generally had one or more peaks in the coarse end of the spectrum, presumably due to the presence of flocs. The fine end ( $< 100 \mu\text{m}$ ) of the spectrum displayed a flat tail with equal concentration of particles in all size classes. Size spectra with this shape indicate that the classical Junge model for description of in situ particle size spectra is reasonable for particles

\*Corresponding author. Present address: School of Ocean Sciences, University of Wales, Bangor, Menai Bridge, Anglesey, LL59 5AB, UK. Tel.: +44 1248 382 274; fax: +44 1248 716 367.

E-mail address: [oss202@Bangor.ac.uk](mailto:oss202@Bangor.ac.uk) (O.A. Mikkelsen).

smaller than 100  $\mu\text{m}$  but not for larger particles. Floc fraction was computed for the merged spectra by using a diameter-to-mass conversion and found to vary between 0.34 and 0.95, within the range reported by other authors.

© 2005 Elsevier Ltd. All rights reserved.

*Keywords:* Underwater photography; Lasers; Particle scattering; Suspended particulate matter; Flocculation; Sediment transport; USA; New Jersey; Newark Bay; Hudson river; 40°45'N; 74°W; Italy; Adriatic sea; Apennine margin; 42°28'N; 14°16'E; 44°48'N; 12°28'E

---

## 1. Introduction

The size spectrum of suspended particles affects fundamentally the transport of mass and transmission of optical and acoustical energy in the sea. The size spectrum is difficult to measure, however, because sizes range from sub-micrometer discrete particles to large, mm-sized loose agglomerations of many small particles often called “flocs”. Accurate characterization of the entire size distribution requires instruments that can resolve small sizes yet still sample over large enough volumes to capture large, rare flocs. Furthermore, because flocs are fragile, observations must be made in situ. Two technologies are applied widely to the direct, in situ measurement of suspended particle size spectra: laser techniques (Bale and Morris, 1987; Law et al., 1997; van der Lee, 1998; Agrawal and Pottsmith, 2000) and photo or video techniques (Milligan, 1996; van Leussen and Cornelisse, 1996; Hill et al., 1998).

Numerous devices have been constructed in various laboratories over the last 2–3 decades to collect images of particles under water (Knowles and Wells, 1996; Maldiney and Mouchel, 1996; Syvitski and Hutton, 1996; Thomsen et al., 1996; Grosjean et al., 2004). These devices have proven useful for characterizing large particles but they tend to have a relatively large lower limit of resolution. The lower limit of resolution depends on the configuration of the camera, and can vary from 4  $\mu\text{m}$  (Eisma et al., 1990) to more than 230  $\mu\text{m}$  (Hill et al., 2001).

One popular group of laser particle sizers is based on the laser diffraction principle. They measure particle size by emitting a laser beam. When the beam encounters a particle it scatters in all directions and thus creates a scattering pattern that includes a forward diffraction pattern related

to the size of particle in question. The forward diffraction pattern is related to the size of the particle in that the peak of the scattered energy occurs at a large angle for small particles and at a small angle for large particles (Agrawal and Pottsmith, 2000). In essence, an ensemble of particles creates a forward diffraction pattern composed of the sum of the diffraction pattern for all the individual particles. The diffraction pattern is detected by a ring detector, measuring the intensity of the scattered light in a number of angles. The scattering pattern can be inverted to yield the particle size distribution under the assumption that the scattering particles are spheres (Agrawal and Pottsmith, 2000).

Currently, existing commercially available in situ laser diffraction techniques can be used to measure floc sizes over a 1:200 dynamic range (Agrawal and Pottsmith, 2000), typically starting at a lower diameter of a few microns, and extending to a maximum upper diameter of a few hundred microns. The LISST series of instruments from Sequoia Scientific, WA, USA, can measure in situ particle size in 32 size bins in a range of sizes: 1.25–250  $\mu\text{m}$  (LISST-100 type B), 2.5–500  $\mu\text{m}$  (LISST-100 type C), or 7.5–1500  $\mu\text{m}$  (LISST-FLOC). Most photographic instruments have a lower limit of resolution of  $\sim 100 \mu\text{m}$ . Therefore, while overlap between the two methods exists, the overall size ranges differ. Neither in situ instrument is able to measure the entire size spectrum of suspended particles in the marine environment. This is unfortunate, as each of the two ends of the particle size spectrum are of importance. Suspended particles with a diameter  $\ll 10 \mu\text{m}$  have a profound influence on the light scattering properties of the water (Stramski and Kiefer, 1991; Ulloa et al., 1994), and the size distribution of particles in the fine end of the size

spectrum is therefore of intrinsic interest to marine optics and remote sensing measurements (Mikkelsen, 2002a; Flory et al., 2004). At the other end of the size spectrum the largest flocs in suspension are of the utmost importance for the deposition of fine-grained particles to the seabed (Van Leussen, 1994).

The importance of characterizing the entire size spectrum has previously spawned efforts to blend the data of different sensors (Jackson et al., 1997). The goal of this work is to assess the feasibility of generating more complete in situ particle size spectra by merging data from a LISST-100 type C, measuring particles in the range 2.5–500  $\mu\text{m}$ , with data from a digital floc camera (DFC) that measures particle sizes larger than 135  $\mu\text{m}$ .

## 2. Materials and methods

The two instruments used to collect data in this study were a LISST-100 type C in situ laser diffraction particle sizer (Agrawal and Pottsmith, 2000) and a DFC (cf. Mikkelsen et al., 2004), which were deployed together at the field sites. Fieldwork was carried out in two locations, the Newark Bay/Hudson River area, NJ, USA, and along the Apennine margin in the Adriatic Sea, off the east coast of Italy. The fieldwork took place in the Newark Bay/Hudson River on 17–18 April 2002 and in the Adriatic Sea in May 2003.

In a LISST-100, the light scattering is detected on 32 ring detectors, the width of which determine the size ranges and the size of the bins of the particle distribution resulting from the inversion process. The raw power count from each ring is stored on a built-in datalogger, offloaded upon retrieval and used for the inversion procedure (Agrawal and Pottsmith, 2000). Light scattered at angles larger or smaller than the angles covered by the ring detectors is not detected. It should be realized that particles smaller than 2.5  $\mu\text{m}$  or larger than 500  $\mu\text{m}$  can still scatter light onto the ring detectors, as each particle creates its own diffraction pattern (cf. above). Therefore, if numerous particles with a size smaller than 2.5  $\mu\text{m}$  or larger than 500  $\mu\text{m}$  are present, excess scatter will occur on the rings associated with the smallest and

largest size bins. Upon inversion of the diffraction pattern this results in an overestimate of particle volume in the smallest and/or largest size bins (Agrawal and Pottsmith, 2000), typically seen as a rising tail in the size spectrum (Mikkelsen, 2002b). In the ideal case, i.e. no excess scattering on the detector rings, the inversion procedure will yield the particle size spectrum in 32 logarithmically spaced size bins ranging 2.5–500  $\mu\text{m}$  (Table 1).

The DFC takes still pictures of the suspended particles by means of silhouette photography whereby the particles are illuminated from behind using a LED flash. The particles thus appear dark on a bright background. The field of view (FOV) is a  $4 \times 4 \times 2.5$  cm slab of water, and the DFC is focused on the middle part of the slab. A small aperture setting and a bright light source ensure that all particles in the FOV are in focus. The LED flash strobes the DFC with a 20  $\mu\text{s}$  pulse. This ensures that the particles in the image are ‘frozen’ and not blurry due to particle movement. The images are stored on an internal hard drive, capable of storing up to 1000 gray scale images with a size of  $1024 \times 1024$  pixels in 256 gray scale values. The pixel size of the camera is 45  $\mu\text{m}$ . In this study, nine coherent pixels were chosen as the minimum number of pixels to define a particle in an image, meaning that the smallest resolvable particle was approximately 135  $\mu\text{m}$ .

Newark Bay and the Hudson River are part of the New York/New Jersey Harbor complex (Fig. 1A). The Hudson River sampling site was in 9 m of water and just south of the George Washington Bridge in the high turbidity zone characterized by Geyer et al. (2001). The anchor station in Newark Bay was in 8 m of water and located in the northern reaches of a dredged channel that provides navigable waters for shipping into the New York/New Jersey Harbor (Fig. 1A).

In Newark Bay and the Hudson River the DFC and the LISST were tied together so they could be lowered on a wire in a profiling mode. The LISST was programmed to measure at 1 Hz, while the DFC measured at 0.25 Hz. Both instruments were pressure-triggered and started measuring when the water pressure exceeded 0.5 dbar. They stopped again when the water pressure dropped below

Table 1

Lower limit, mid point and upper limit in microns for size bins 1–32 (**bold**, covered by the LISST) and size bins 25–50 (*italic*, covered by the DFC). The two instruments are seen to overlap in eight size bins, 25–32

Size bin #	Lower limit ( $\mu\text{m}$ )	Mid point ( $\mu\text{m}$ )	Upper limit ( $\mu\text{m}$ )	Size bin #	Lower limit ( $\mu\text{m}$ )	Mid point ( $\mu\text{m}$ )	Upper limit ( $\mu\text{m}$ )
1	<b>2.50</b>	<b>2.72</b>	<b>2.95</b>	26	<i>156.90</i>	<i>170.44</i>	<i>185.15</i>
2	<b>2.95</b>	<b>3.20</b>	<b>3.48</b>	27	<i>185.15</i>	<i>201.13</i>	<i>218.49</i>
3	<b>3.48</b>	<b>3.78</b>	<b>4.11</b>	28	<i>218.49</i>	<i>237.35</i>	<i>257.83</i>
4	<b>4.11</b>	<b>4.46</b>	<b>4.85</b>	29	<i>257.83</i>	<i>280.09</i>	<i>304.26</i>
5	<b>4.85</b>	<b>5.27</b>	<b>5.72</b>	30	<i>304.26</i>	<i>330.52</i>	<i>359.05</i>
6	<b>5.72</b>	<b>6.21</b>	<b>6.75</b>	31	<i>359.05</i>	<i>390.04</i>	<i>423.70</i>
7	<b>6.75</b>	<b>7.33</b>	<b>7.97</b>	32	<i>423.70</i>	<i>460.27</i>	<i>500.00</i>
8	<b>7.97</b>	<b>8.65</b>	<b>9.40</b>	33	<i>500.00</i>	<i>543.15</i>	<i>590.03</i>
9	<b>9.40</b>	<b>10.21</b>	<b>11.09</b>	34	<i>590.03</i>	<i>640.96</i>	<i>696.28</i>
10	<b>11.09</b>	<b>12.05</b>	<b>13.09</b>	35	<i>696.28</i>	<i>756.38</i>	<i>821.66</i>
11	<b>13.09</b>	<b>14.22</b>	<b>15.45</b>	36	<i>821.66</i>	<i>892.58</i>	<i>969.61</i>
12	<b>15.45</b>	<b>16.78</b>	<b>18.23</b>	37	<i>969.61</i>	<i>1053.30</i>	<i>1144.20</i>
13	<b>18.23</b>	<b>19.81</b>	<b>21.52</b>	38	<i>1144.20</i>	<i>1243.00</i>	<i>1350.20</i>
14	<b>21.52</b>	<b>23.37</b>	<b>25.39</b>	39	<i>1350.20</i>	<i>1466.80</i>	<i>1593.40</i>
15	<b>25.39</b>	<b>27.58</b>	<b>29.96</b>	40	<i>1593.40</i>	<i>1730.90</i>	<i>1880.30</i>
16	<b>29.96</b>	<b>32.55</b>	<b>35.36</b>	41	<i>1880.30</i>	<i>2042.60</i>	<i>2218.90</i>
17	<b>35.36</b>	<b>38.41</b>	<b>41.72</b>	42	<i>2218.90</i>	<i>2410.40</i>	<i>2618.40</i>
18	<b>41.72</b>	<b>45.32</b>	<b>49.23</b>	43	<i>2618.40</i>	<i>2844.40</i>	<i>3089.90</i>
19	<b>49.23</b>	<b>53.48</b>	<b>58.10</b>	44	<i>3089.90</i>	<i>3356.60</i>	<i>3646.30</i>
20	<b>58.10</b>	<b>63.12</b>	<b>68.56</b>	45	<i>3646.30</i>	<i>3961.00</i>	<i>4302.90</i>
21	<b>68.56</b>	<b>74.48</b>	<b>80.91</b>	46	<i>4302.90</i>	<i>4674.30</i>	<i>5077.70</i>
22	<b>80.91</b>	<b>87.89</b>	<b>95.48</b>	47	<i>5077.70</i>	<i>5516.00</i>	<i>5992.10</i>
23	<b>95.48</b>	<b>103.72</b>	<b>112.67</b>	48	<i>5992.10</i>	<i>6509.30</i>	<i>7071.10</i>
24	<b>112.67</b>	<b>122.39</b>	<b>132.96</b>	49	<i>7071.10</i>	<i>7681.40</i>	<i>8344.30</i>
25	<b>132.96</b>	<b>144.43</b>	<b>156.90</b>	50	<i>8344.30</i>	<i>9064.50</i>	<i>9846.90</i>

0.5 dbar upon retrieval. A total of 18 profiles were measured at the two anchor stations. During profiling the instruments were frequently kept at a constant depth for 10–30 s, in order to obtain multiple measurements of particle size in the same water mass.

The fieldwork in the Adriatic Sea was carried out as part of the ONR-supported EuroSTRATAFORM project, which was concerned with sedimentary processes and the development of sedimentary strata in the vicinity of the Po River and on the Apennine margin. As part of EuroSTRATAFORM a newly designed tripod, INSSECT (Mikkelsen et al., 2004), was deployed along the Apennine margin on several occasions during a research cruise in May/June 2003. The purpose of the INSSECT deployments was to characterize the temporal and spatial variations in suspended particle characteristics such as size and

settling velocity along the margin. The INSSECT rotates in the current, so the instruments are perpendicular to the flow of water. In this way disruption of flocs due to turbulence around the instrumentation is minimized (Mikkelsen et al., 2004). The deployments had durations of 8–72 h, and the DFC was programmed to take a picture every 5 or 10 min depending on the length of the deployment. The LISST was programmed to start when the pressure exceeded 0.5 dbar. Its sampling frequency was 4 Hz in a burst mode, with a burst every five minutes. For each burst, five samples with a sample interval of five seconds were stored, each sample being an average of 10 individual 4 Hz measurements. Measurements in the Adriatic were carried out in water depths of 9–14 m off the Po, Chienti, and Pescara Rivers (Fig. 1B). Table 2 summarizes the DFC and LISST data that were collected for the various locations.

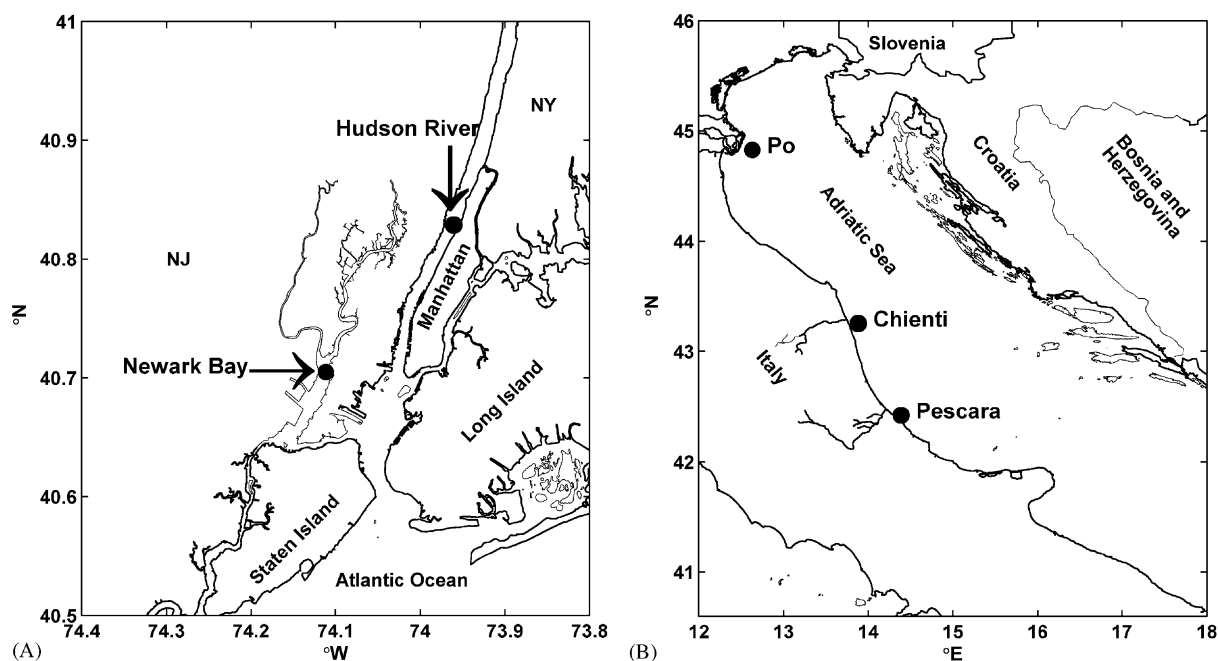


Fig. 1. (A) Map of Newark Bay/Hudson River area showing the anchor stations in Newark Bay and The Hudson River. (B) Map of the Adriatic showing the location of the INSSECT deployments off the rivers Po, Chienti, and Pescara.

Table 2

Dates, times, positions, water depths and number of DFC and LISST measurements for the fieldwork sites

	Date and time (UTC)	Lat, Long	Depth (m)	DFC images	LISST measurements
Po	19:25 25 May–17:15 26 May 2003	42°27.8N, 14°16.0E	12	248	1240
Chienti	16:10 22 May–15:55 24 May 2003	43°17.7N, 13°45.6E	10	276	1380
Pescara	10:35 30 May–11:20 31 May 2003	44°47.8N, 12°27.8E	10	263	1315
Newark Bay	13:59–20:08 17 April 2002 & 13:10–14:10 18 April 2002	40°42.2N, 74°7.0W	8	834 (14 profiles)	3657
Hudson River	18:28–20:11 18 April 2002	40°49.5N, 73°58.1W	8	197 (4 profiles)	557

Upon retrieval of the LISST-100 and the DFC, data were offloaded and a number of post-processing steps carried out in order to obtain particle volume distributions from each instrument. The raw LISST-100 data were inverted using manufacturer-supplied software. This inversion yields the volume distribution of suspended particles. Multiplication of the volume distribution with a volume conversion coefficient yields the absolute volume concentration ( $VC$ ) in each size bin. The volume conversion coefficient is obtained

by a factory calibration whereby the scattering pattern of particles with known sizes and volume concentrations are measured. Details regarding the entire procedure can be found in Agrawal and Pottsmith (2000) as well as Traykovski et al. (1999). The final output from the LISST-100 is the volume distribution in 32 logarithmically spaced size bins.

DFC images were analyzed using the MATLAB Image Processing Toolbox. For each image, an area of interest (AOI) was selected, and all

particles in the AOI were initially discriminated from the background using Otsu's method (Otsu, 1979), which automatically selected a threshold level. A binarized image of the AOI was then produced. Upon evaluation of this image the analyst could change the threshold if needed. All images from a deployment were then binarized automatically using this threshold. For each image, every particle in the AOI was counted, and the area of each particle was computed. Particle volumes and diameters were computed under the assumption that the particles were spheres. Finally, particle volumes were binned into 50 logarithmically increasing size bins.

The size bins for the two instruments are shown in Table 1. The LISST measures in size bins 1–32 (2.5–500  $\mu\text{m}$ ), while the DFC measures particles larger than 135  $\mu\text{m}$  (size bins 25 and larger). The instruments overlap in size bins (25–32), or the size range 135–500  $\mu\text{m}$ . When analyzing data obtained with the DFC, the analyst is free to choose the size and limits of the size bins. For this study, the DFC size bins were chosen so that they would match and extend the LISST size bins. The maximum particle size that can be measured by the DFC is in principle only limited by the slab width of the DFC (2.5 cm). However, flocs larger than 2000  $\mu\text{m}$  are seldom observed, so for the image analysis procedure the number of size bins in the DFC was arbitrarily set to 50, giving a maximum particle size of 9900  $\mu\text{m}$  (Table 1). Since the smallest particle resolvable by the LISST-100 is 2.5  $\mu\text{m}$ , this gives a dynamic range of roughly 1:4000 (2.5–9900  $\mu\text{m}$ ).

For the data obtained in Newark Bay and the Hudson River, only the measurements obtained while the instruments were kept at a constant depth during profiling were used. The rationale for limiting analysis to these times is that the LISST and the DFC pressure sensors were offset. This offset made it difficult to compare individual measurements. Another complicating factor was the fact the DFC measured at 0.25 Hz while the LISST measured at 1 Hz. Typically, 10–50 LISST measurements (average: 30) and 3–10 DFC images (average: 6) were obtained at each depth. The size spectra from each constant level were averaged into one size spectrum for each instrument.

For the DFC and LISST data obtained in the Adriatic Sea, the five LISST samples making up one burst were averaged into one spectrum. This spectrum was then compared to the DFC spectrum obtained from the DFC image taken at the same time as the LISST burst.

From the frequency volume distributions, cumulative relative frequencies were computed and the first, second, and third quartiles were determined. The particle diameters associated with these three quartiles are denoted  $D_{75}$ ,  $D_{50}$  and  $D_{25}$ , respectively.  $D_{75}$  is the lower quartile diameter, i.e. 75% of the particle volume is contained in particles larger than  $D_{75}$ .  $D_{50}$  is the median particle diameter, and  $D_{25}$  is the upper quartile diameter.

For both instruments, values for  $D_{75}$ ,  $D_{50}$ , and  $D_{25}$  were also computed using only the volume distribution in the eight overlapping size bins. In the following these diameters are referred to as “trimmed diameters”. Trimmed diameters were computed for size bins 25–32, 25–31, 25–30, 25–29, and 25–28. Thus, they are diameters that are representative for particles in the size ranges 135–500, 135–424, 135–359, 135–304, and 135–258  $\mu\text{m}$  only.

### 3. Results

The relative response of the two instruments was different in the two main locations. In the Adriatic Sea, median diameters estimated with the LISST were 2–3 times smaller than those estimated with the DFC (Fig. 2A). This difference is attributable to the different size ranges measured by the two devices. Despite this difference, temporal trends measured by the instruments were similar. For example, near the Chienti River maximum values of  $D_{50}$  occurred around 0000 on 23 May and 0300 on 24 May, and minimum values occurred around 0600 on 23 May and 0900 on 24 May (Fig. 2A). The differences between LISST and DFC values of  $D_{50}$  largely disappeared when trimmed diameters, computed using size bins 25–32 (135–500  $\mu\text{m}$ ), were compared (Fig. 2B).

The variation in  $D_{50}$  and trimmed  $D_{50}$  for the data obtained in Newark Bay demonstrated a

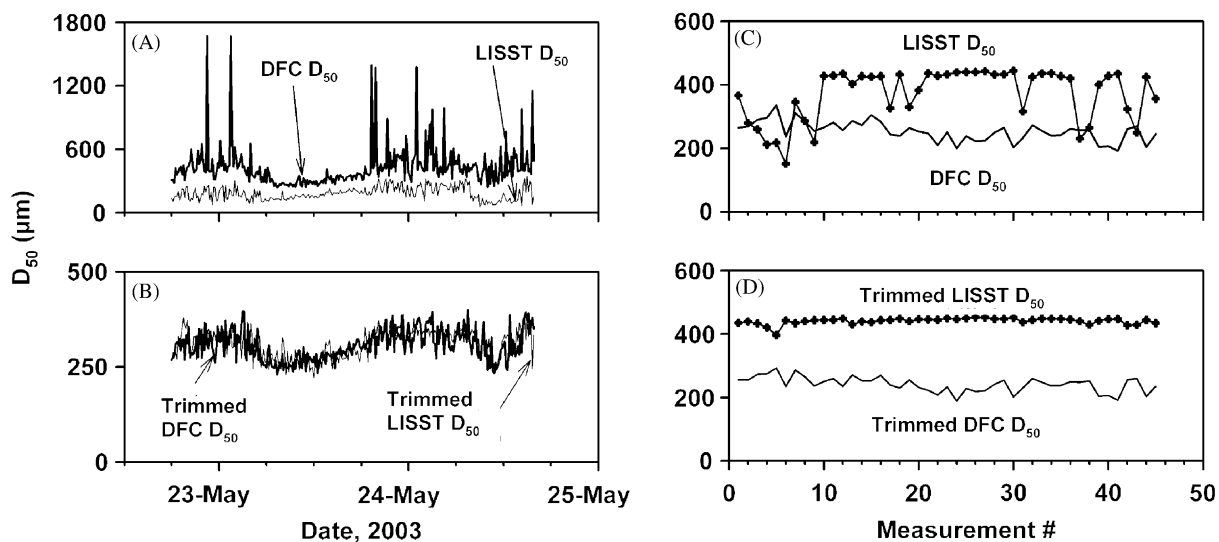


Fig. 2. Temporal variation in  $D_{50}$  and trimmed  $D_{50}$  from the DFC and the LISST off the Chienti River (A,B), and at the Newark Bay anchor station (C,D). (A,C)  $D_{50}$  computed for all size bins from each of the two instruments, i.e. bins 1–32 for the LISST and 25–50 for the DFC (cf. Table 1). (B,D) Trimmed  $D_{50}$ , computed using only the overlapping size bins (25–32, cf. Table 1).

pattern different from the one observed in the Chienti deployment (Figs. 2C and D). Both instruments recorded almost constant values for  $D_{50}$  as well as for trimmed  $D_{50}$ , with the LISST showing the highest values and the least variation. The results from the Po and Pescara Rivers were similar to the Chienti results, while the results from the Hudson River were similar to the results from the Newark Bay (data not shown).

The agreement between values of  $D_{75}$ ,  $D_{50}$ , and  $D_{25}$  estimated with the two instruments depended on deployment site and on the number of bins used to calculate trimmed quartile diameters. For the deployments in the Adriatic Sea, all trimmed quartile diameters plotted within one standard deviation of the 1:1 line (Fig. 3A–C). For the Newark Bay anchor station (Fig. 3D), the trimmed quartiles plotted within one standard deviation of the 1:1 line only if bin 32 was removed. For the Hudson River anchor station (Fig. 3E), also size bin 31 had to be omitted before the trimmed quartiles began to plot within one standard deviation of the 1:1 line. Apparently, in Newark Bay and the Hudson River the largest LISST size bins were responsible for disagreement between trimmed quartile diameters.

Both instruments produced estimates of absolute  $VC$  in each size bin. Linear relationships between the  $VC$  in individual size bins were evident (Figs. 4 and 5). However, compared to the DFC, the LISST provided lower estimates for  $VC$ . In order to quantify the disagreement between the two instruments, the slope for each of the eight volume:volume relationships was computed for all deployments. For each deployment the eight values for the slope were averaged, and the standard deviation was computed (Table 3). The average slope gave an estimate of the overall offset between the DFC volume and the LISST volume. The DFC volume was up to a factor of 8.5 higher than the LISST volume (the Po River), but more commonly was higher by about a factor of 3.

The fact that linear volume:volume relationships existed between the instruments made it possible to adjust the volumes in the overlapping bins to each other simply by applying a suitable correction factor. Subsequently, the LISST spectrum in size bins 24 and smaller or the DFC spectrum in bins 33 and larger was then corrected. In order to do this, the volumes in the overlapping bins had to be adjusted so that either the LISST volume was corrected to the DFC volume or the DFC volume

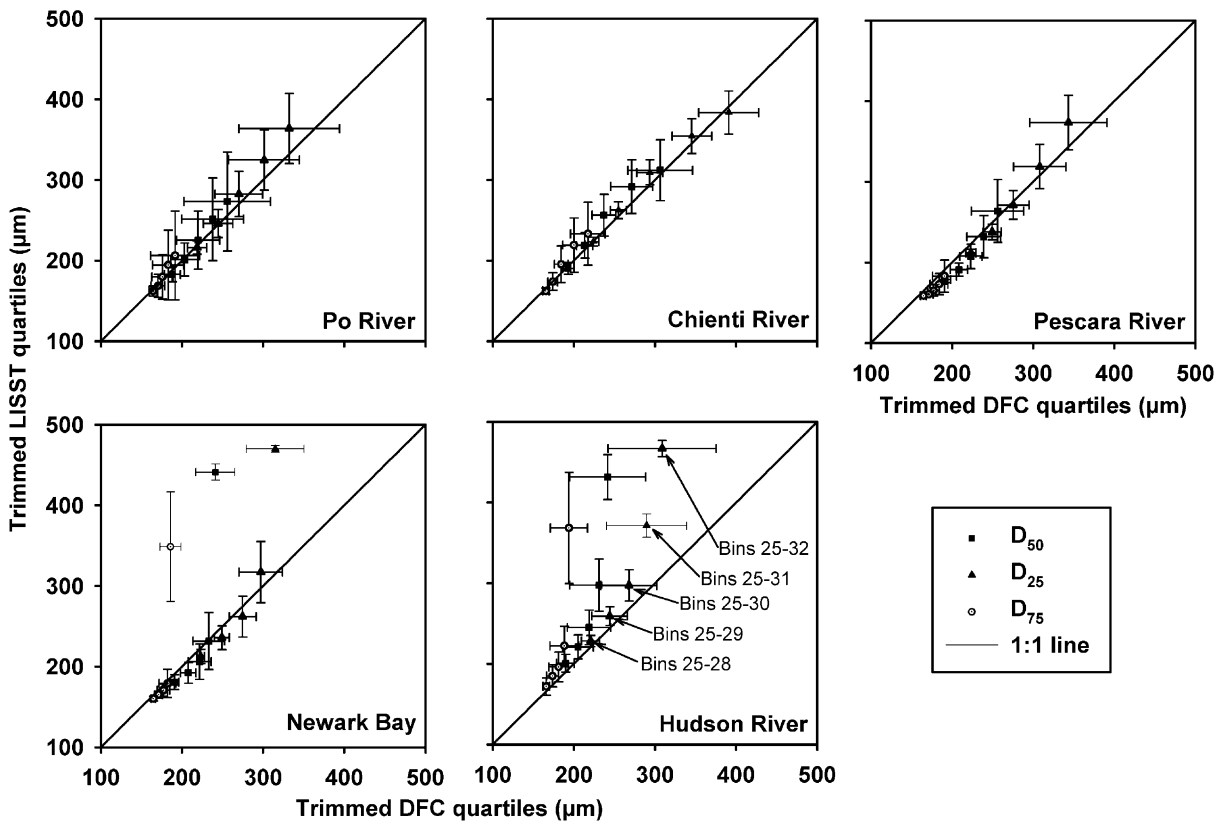


Fig. 3. Comparison of the mean values of the trimmed quartile diameters. Symbols denote the different quartiles. For each quartile, five points are plotted. The largest of the 5 shows the quartile diameter when bins 25–32 were used in the calculation, while the least of the 5 shows the quartile diameter when bins 25–28 were used. The intermediate points used, in increasing order, bins 25–29, 25–30, and 25–31. Error bars show  $\pm$  one standard deviation.

was corrected to the LISST volume. Regardless of which size spectrum was being adjusted, it was important to use only one correction factor for all bins in the spectrum. If a different correction factor had been used for each bin, the shape of the adjusted spectrum would have differed from the original spectrum.

In the following a method for adjusting LISST spectra to DFC spectra is described. This is not to be taken as an indication of which instrument is believed to measure the volume distribution of suspended matter most accurately. One instrument simply has to be chosen as the reference instrument to which the other is adjusted, and in this study the DFC was chosen as the reference. It is important to bear in mind that it has no

implications for the resulting shape of the particle size distribution which instrument is chosen as a reference.

For every LISST spectrum and its corresponding DFC spectrum, the offset ratio between the LISST volume and the DFC volume was computed for the maximum number of bins that plotted within one standard deviation of the 1:1 line on Fig. 3. In this way, offset ratios for each pair of size spectra were computed for bins 25–32 for all data from the Adriatic, for bins 25–31 for the data from Newark Bay and for bins 25–30 for the data from the Hudson River. For each pair of spectra, the median value of the ratios was computed. Then, all bins in the LISST size spectrum were multiplied by the median value of

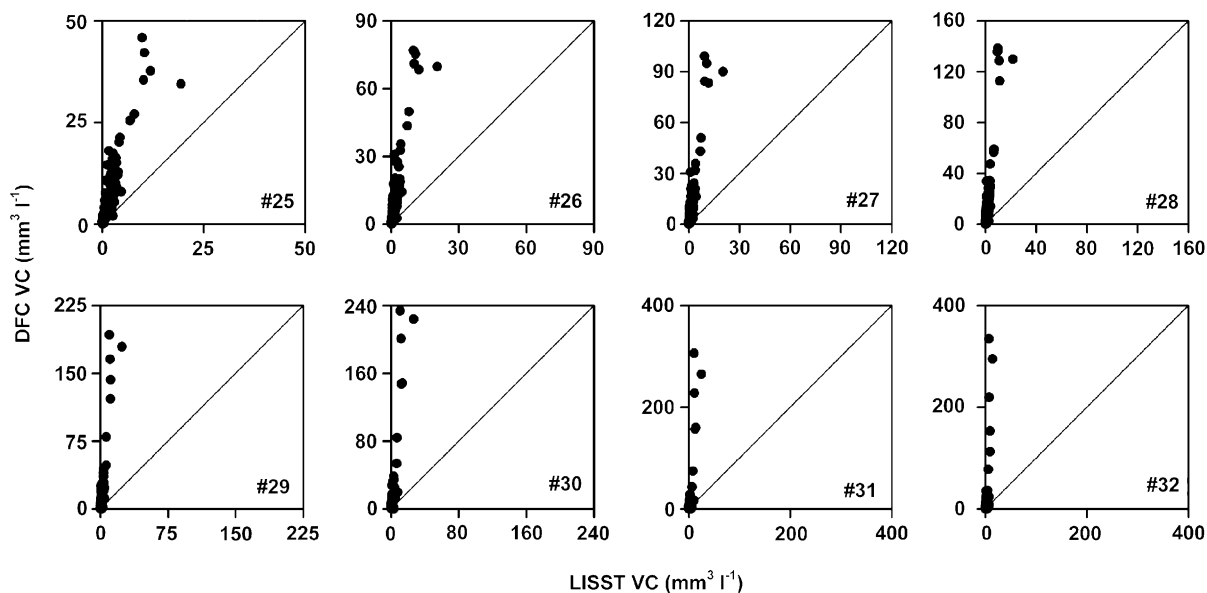


Fig. 4. Relationships between the volume concentration ( $VC$ ) from the DFC and the LISST for each of the eight overlapping size bins; #25–32. Data are from the Po. Also shown are the 1:1 lines.

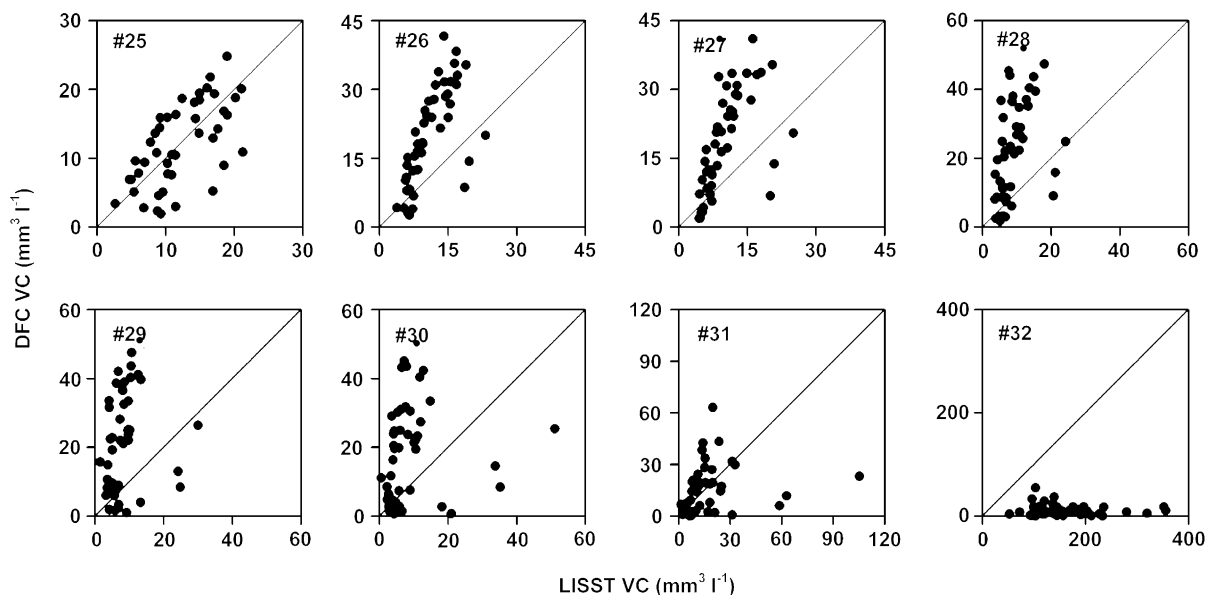


Fig. 5. Relationships between the volume concentration ( $VC$ ) from the DFC and the LISST for each of the eight overlapping size bins; #25–32. Data are from Newark Bay anchor Station. Also shown are the 1:1 lines.

the ratios. This value varied between 0.2 and 24.5, with an overall average value of 4.1 ( $n = 1818$ ). This procedure adjusted the magnitude of the

entire LISST volume distribution so that it was of equivalent magnitude to the corresponding DFC distribution in the region of overlap without

changing the shape of the LISST spectrum. With this method the corrected volume:volume relationships for the data from off the Po river and from the Newark Bay anchor station generally plotted along a 1:1 line (Figs. 6 and 7). Mean slopes for the corrected relationships were all near unity (Table 4).

Upon correction of the volumes in the overlapping size bins a merged spectrum was obtained in the following manner. Volumes in bins 1–24 of the merged spectrum were set equal to the volumes

in bins 1–24 from the corrected LISST spectrum, and volumes in bins 33–50 of the merged spectrum were set equal to the volumes in bins 33–50 from the DFC spectrum. The merging of bins 25–32 differed, depending on which bins were used for the LISST volume correction procedure. If some bins (e.g. bins 31 and 32 in the case of the Hudson River) were not used in the volume correction procedure, then these bins in the merged spectrum were assigned the volumes from the same bins in the corresponding DFC spectrum. For the bins that were used to correct the volume (e.g. 25–30 for the Hudson River), the volumes were assigned the average value of the corrected LISST spectrum and the DFC spectrum. In this manner a size spectrum covering the entire size range from 2.5  $\mu\text{m}$  and up was obtained, and  $D_{75}$ ,  $D_{50}$  and  $D_{25}$  for the merged spectrum were computed.

Fig. 8 shows examples of merged size spectra together with the original LISST and DFC spectrum used to create the merged spectrum. The spectra were selected so that they were spread evenly throughout each deployment. Table 5 contains more detailed information with respect to the timing, location, depth and  $D_{50}$  for each of

Table 3  
Mean and standard deviation for the slope between the volume concentration in the uncorrected LISST bins and the DFC bins

	Po	Chienti	Pescara	Newark Bay	Hudson river
Mean slope	8.5	3.4	3.3	1.1	-0.3
Std slope	4.0	1.1	1.6	0.9	0.1
Bins used	25–32	25–32	25–32	25–31	25–30

A slope was computed for the overlapping bins (cf. Figs. 4–7). The mean slope tabulated here is the average from each location of these 6–8 values. Bins used were determined from Fig. 3 (see text relating to Fig. 3 for explanation).

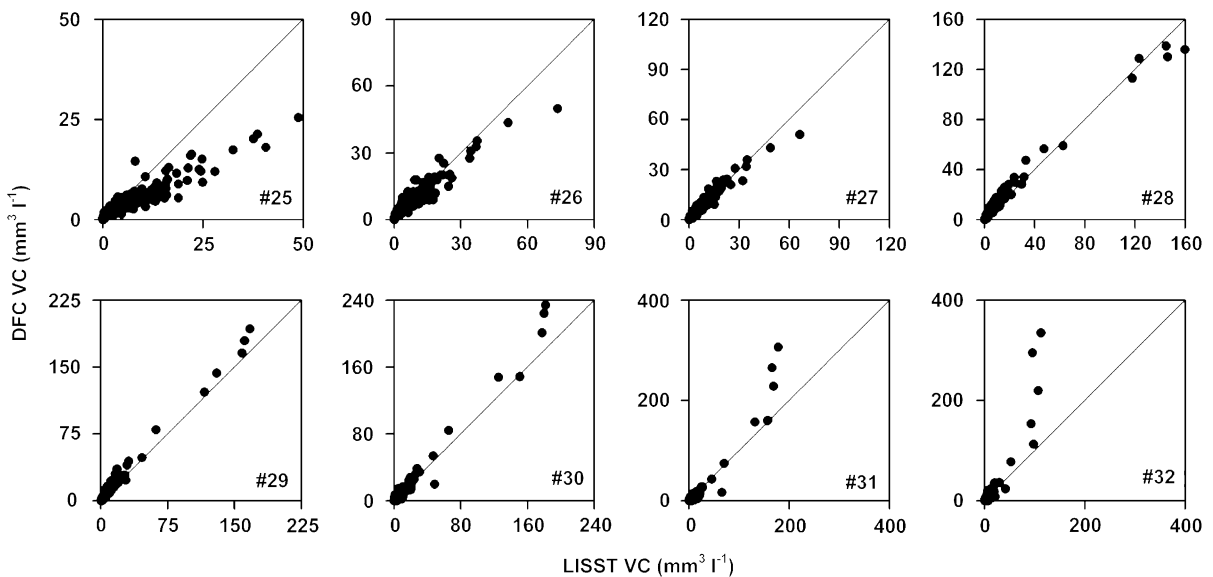


Fig. 6. Relationships between the volume concentration ( $VC$ ) from the DFC and the corrected LISST volume for each of the eight overlapping size bins; #25–32. Data are from the Po. Also shown are the 1:1 lines.

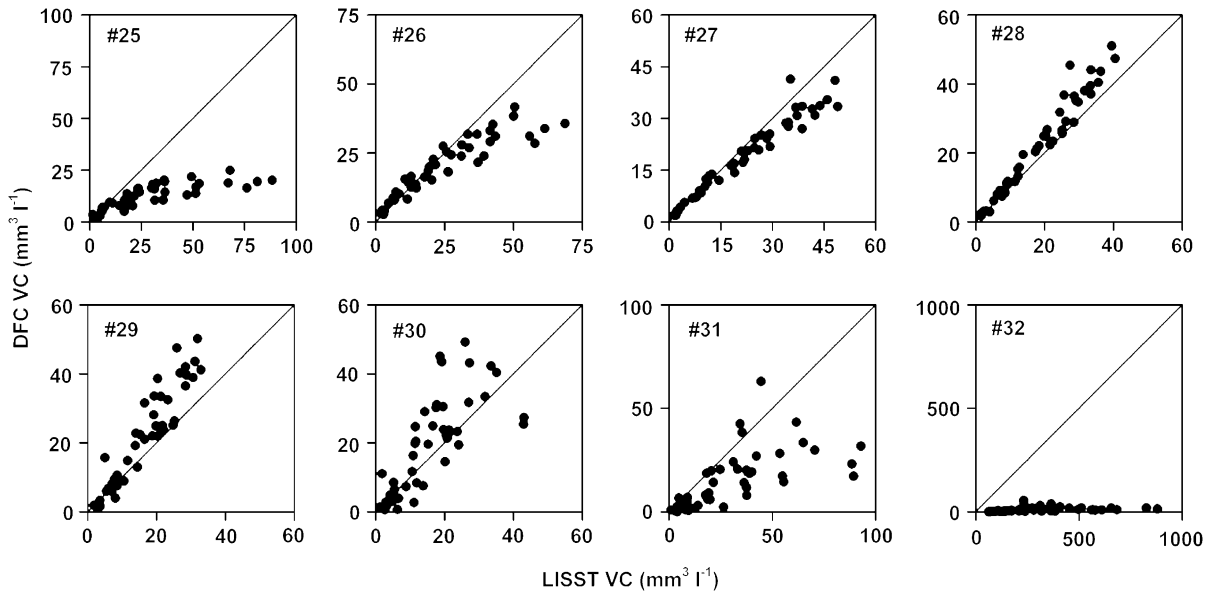


Fig. 7. Relationships between the volume concentration ( $VC$ ) from the DFC and the corrected LISST volume for each of the eight overlapping size bins; #25–32. Data are from Newark Bay anchor station. Also shown are the 1:1 lines.

Table 4

As for Table 3, but showing the mean and standard deviation for the slope between the volume concentration in the volume corrected LISST bins and the DFC bins

	Po	Chienti	Pescara	Newark Bay	Hudson river
Mean slope	1.0	0.9	0.8	0.7	0.6
Std slope	0.5	0.2	0.4	0.4	0.2
Bins used	25–32	25–32	25–32	25–31	25–30

the spectra shown in Fig. 8. Many of the spectra have a flat tail in the finer portion and a distinct mode or modes in the coarser end.

#### 4. Discussion

Two factors complicated the merging of LISST and DFC data. First, for some deployments the LISST assigned large volumes to its upper size bin(s), causing degradation in the match between LISST and DFC size spectra. Second, LISST sensed less particle volume in the water than the DFC.

Whenever particles larger than  $500\ \mu\text{m}$  are present in the LISST sensing volume, they will scatter some light onto the innermost ring detectors (Agrawal and Pottsmith, 2000). Under these circumstances the additional light will be detected and interpreted by the LISST as extra particle surface area in the largest bin(s). The volume in the bin(s) is then overestimated, causing a coarse “rising tail” in the size spectrum (cf. Figs. 8J–O). This problem causes the LISST  $D_{75}$ ,  $D_{50}$  and  $D_{25}$  to be overestimated. A rising tail can occur if as little as 4% of the total particle volume is outside the size range of the instrument (Mikkelsen, 2002b). Rising tails were observed in almost every LISST spectrum from Newark Bay and the Hudson River (cf. Fig. 8J–O), but generally not for the spectra from the Adriatic.

While rising tails in the size spectrum cause the LISST  $D_{75}$ ,  $D_{50}$  and  $D_{25}$  to increase, the influence can be mitigated by omitting the size bins with the rising tails, and re-computing the diameter. In this way reliable particle diameters for the part of the distribution not affected by the rising tails can be obtained (Fig. 3).

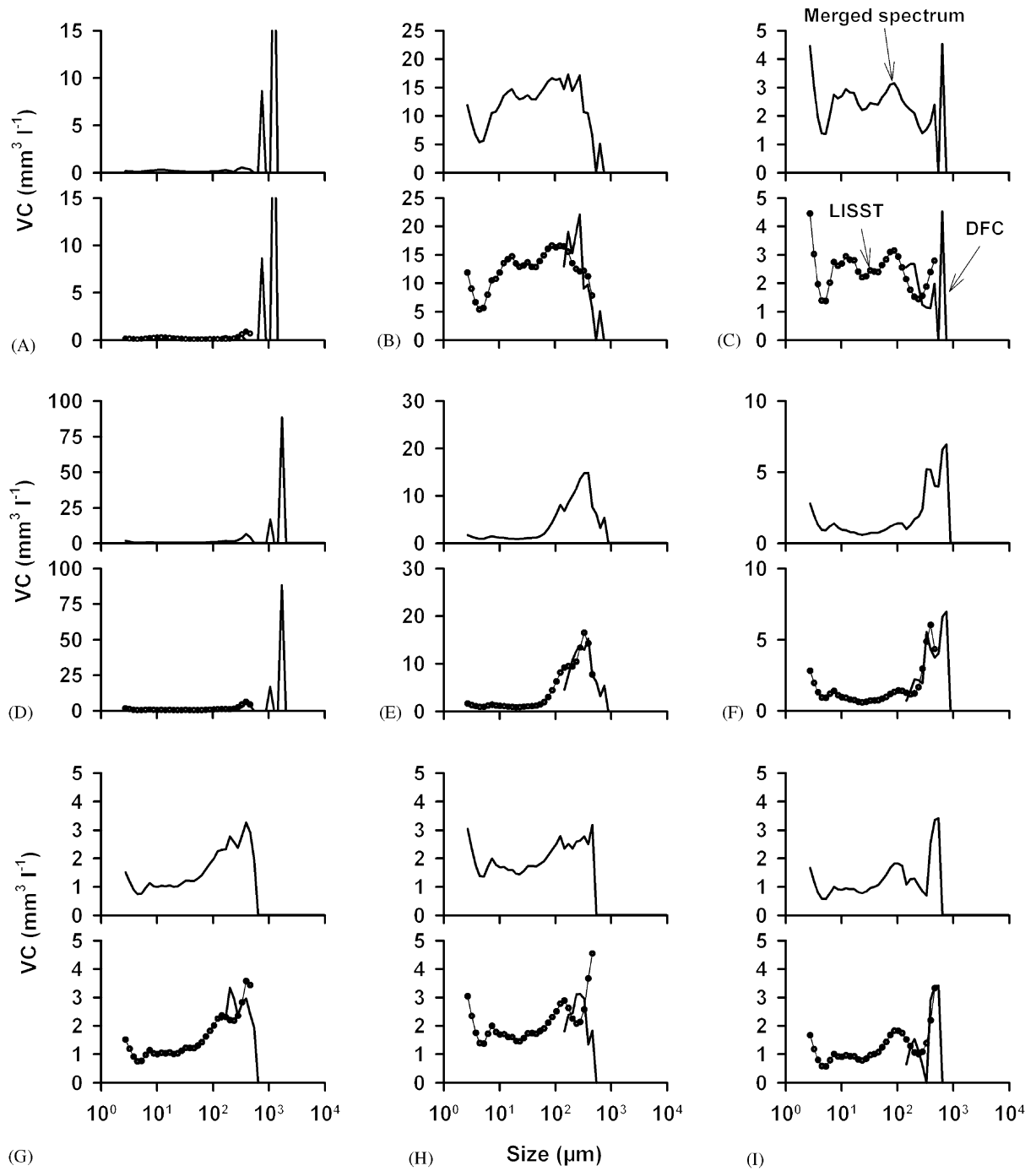


Fig. 8. Examples of merged size spectra (top graph in each panel) together with the DFC spectra and the volume corrected LISST spectra used for the merging procedure (bottom graph in each panel). (A–C) are off the Po River, (D–F) off the Chienti River, (G–I) off the Pescara River, (J–L) from Newark Bay anchor station and (M–O) from the Hudson River anchor station. See Table 5 for details regarding the individual spectra.

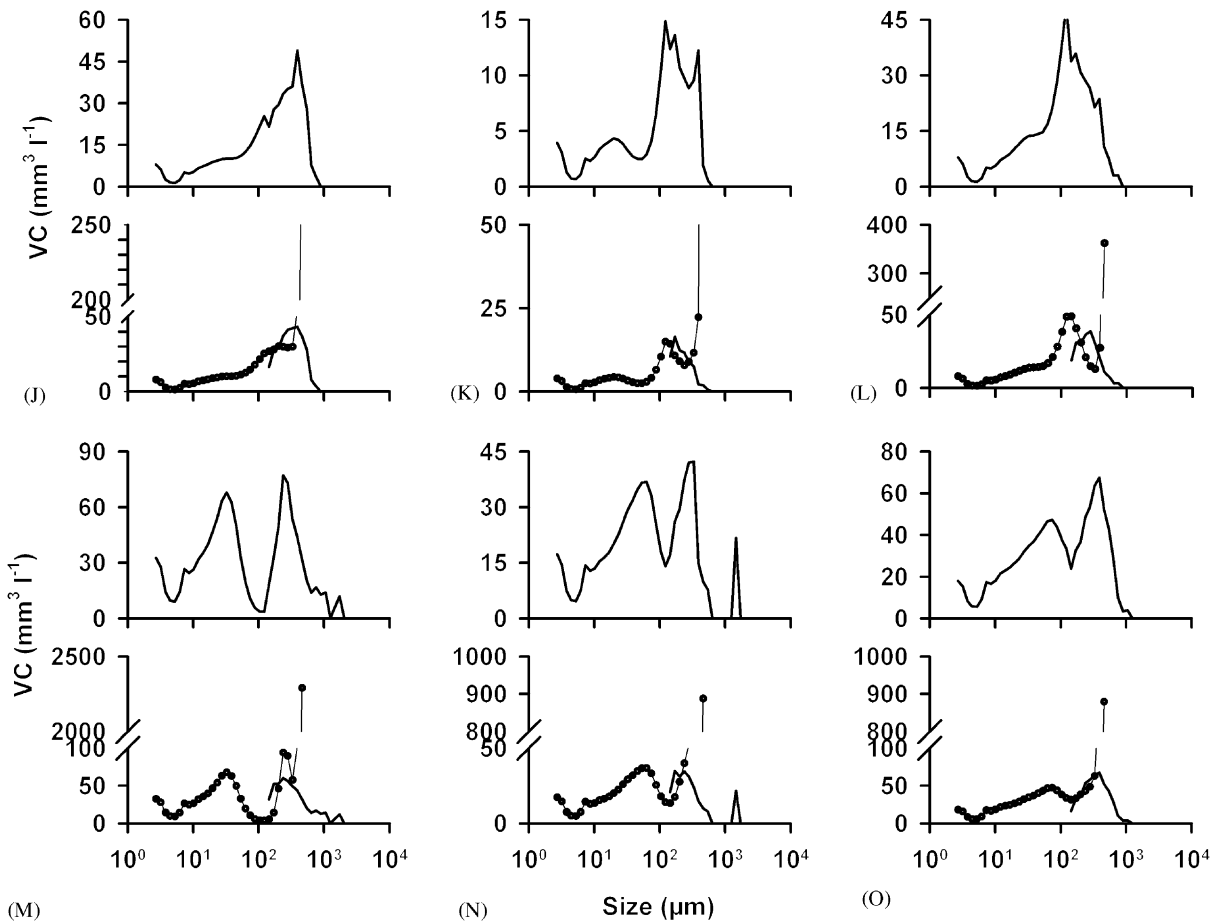


Fig. 8. (Continued)

While the volume variation between bins without a rising tail was similar between instruments, the absolute  $VC$  in the same size bins differed (Figs. 4 and 5). The LISST and the DFC volumes were at times offset by almost one order of magnitude prior to correction (cf. Table 3); however, discrepancies of a factor of  $\sim 3$  or less were more common. Even so, a discrepancy of this size between the two instruments was unexpected. Assuming that the actual volume concentrations were somewhere in between the LISST and the DFC volume measurements, then the total volume concentrations derived from merged spectra can only be correct to within one order of magnitude. This is a matter of concern because the in situ volume distribution of particles in the sea affects

transmission of energy as well as the transport of mass. Studies concerned with the optical properties of the water or sedimentation of organic and inorganic mass rely to some degree on knowledge of the volume concentration and distribution of particles in situ. It should be realized that this has only minute implications for the computation of particle size based on the volume distribution. It was shown that the shape of the size spectra in the region of overlap was the same (Figs. 4–7), regardless of the discrepancy in actual volume. A constant correction factor was applied to match the LISST volume distribution with the DFC volume distribution in the region of overlap, assuring that the shape of the LISST spectra did not change. Therefore the volume adjustment of

Table 5  
Details for the merged size spectra shown in Fig. 8

Spectrum	Location	Time and date (UTC)	Water depth (m)	Sample depth (m)	LISST $D_{50}$ ( $\mu\text{m}$ )	DFC $D_{50}$ ( $\mu\text{m}$ )	Merged $D_{50}$ ( $\mu\text{m}$ )
A	Po	22:52; 25 May 2003	13.4	11.8	67	1208	1192
B	—	05:47; 26 May 2003	13.5	11.9	48	242	51
C	—	12:37; 26 May 2003	13.2	11.6	32	261	38
D	Chienti	01:30; 23 May 2003	9.5	7.9	209	1670	1645
E	—	16:50; 23 May 2003	9.6	8.0	198	307	228
F	—	08:10; 24 May 2003	9.4	7.8	113	454	280
G	Pescara	14:56; 30 May 2003	12.3	10.7	96	273	104
H	—	22:16; 30 May 2003	12.0	10.4	60	254	56
I	—	05:36; 31 May 2003	11.9	10.3	70	409	80
J	Newark Bay	15:26; 17 May 2002	7.6	7.4	345	311	179
K	—	18:10; 17 May 2002	7.7	7.6	428	209	124
L	—	20:07; 17 May 2002	9.1	2.0	230	256	116
M	Hudson River	18:32; 18 May 2002	9.1	6.1	442	290	43
N	—	19:11; 18 May 2002	8.6	3.8	427	251	62
O	—	20:08; 18 May 2002	8.4	2.2	388	336	91

the LISST data does not affect computation of the size of the particles detected by the LISST or from a merged spectrum.

Several factors may have been responsible for disagreement between instruments. The factory-calibrated volume conversion coefficient may have been in error. Edge detection issues in DFC image analysis may have caused misrepresentations of particle size. The different sizes of the sampling volumes of the two instruments may have caused disagreement when large particles were rare. The laser in the LISST may have been misaligned. And finally, particle overlap in the sensing volumes of the instruments may have caused misrepresentations of particle size. Each of these possible sources of disagreement is examined briefly below.

The scattering intensity on each of the ring detectors is proportional to the total surface area of particles within the size range covered by the detector in question. In order to obtain the particulate volume concentration for each ring, the scattering intensity is multiplied with a factory calibration factor. This calibration factor is derived in the laboratory using spherical particles of a known size and volume concentration; see Agrawal and Pottsmith (2000) for details. The volume calibration constant differs between instruments, but is constant for each instrument

throughout its size range. However, in a series of laboratory experiments, Gartner et al. (2001) found the volume conversion factor to vary by a factor of roughly three, but could not provide any explanation for the variation. In contrast, Traykovski et al. (1999) and Agrawal and Pottsmith (2000) showed the volume conversion to be constant for a range of size distributions. Conceivably, there might have been some variation in the LISST volume conversion coefficient across the size range which could explain some of the discrepancy in the volume concentration.

Chen and Eisma (1995) demonstrated the influence of the thresholding value for analyzing digital images. They repeatedly analyzed an image using different threshold values for separating flocs from the background and found that variations in threshold could cause variations in number concentration as well as the final size of the flocs. The number of particles detected in the image was shown to vary by a factor of three, between 250 and 750, while the mean floc size was shown to vary between 155 and 185  $\mu\text{m}$ . Chen and Eisma (1995) did not report on variations in particle volume as a function of changing threshold. Therefore a DFC image from the deployment off the Chienti River was analyzed repeatedly with varying threshold values. The number concentration

of particles ( $NC$ ), the total volume concentration ( $VC_{tot}$ ) and the  $D_{50}$  were determined with the threshold level increasing in steps of three between each analysis (Fig. 9).  $D_{50}$  was not to be affected to any great extent, varying only 10%, between 300 and 330  $\mu\text{m}$ . However,  $NC$  and  $VC_{tot}$  varied by up to a factor of 2–3 for realistic variations in the threshold level.

In this study, the same threshold value was used for all images originating from one deployment. Changes in the overall darkness of the images were occasionally observed, related to changes in overall suspended particulate matter concentration, which varied due to resuspension, settling, and advection. Changes in suspended particulate matter concentration caused images to appear darker or brighter overall. Using a constant threshold on a series of images with varying darkness was

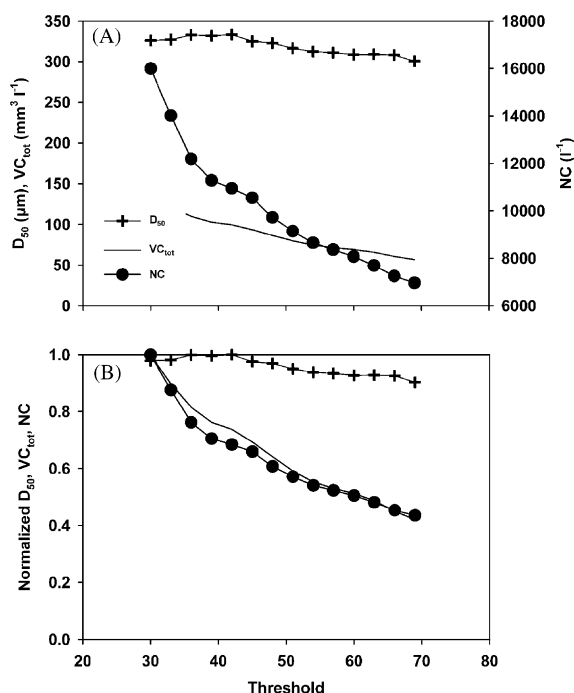


Fig. 9. Changes in the number concentration ( $NC$ ) of flocs in an image, together with changes in the total volume concentration ( $VC_{tot}$ ) and median diameter ( $D_{50}$ ) as a function of threshold level. (A) Absolute changes. (B) Relative changes.  $D_{50}$  was not affected by changes in the threshold while the number and volume concentration of the flocs increased with decreasing threshold. Image used was # 130 off the Chienti River, taken at 15:40 UTC, 23 May 2003.

equivalent to varying the threshold for images with constant darkness and could have caused the same variation in  $D_{50}$ . Therefore, image analysis procedures cannot be ruled out as the source of discrepancy between particle volumes estimated with the LISST and with the DFC.

The DFC and the LISST have sensing volumes with different sizes. The DFC measurement volume is approximately  $40 \text{ cm}^3$  while the LISST-100 measurement volume is  $1.4 \text{ cm}^3$ , a difference of 28 times. The probability of the occurrence of a large particle of a given size in the DFC volume was much larger than the probability of a particle of the same size being present in the LISST volume. For individual LISST measurements, rarity of large particles combined with a small sensing volume would have caused the LISST to underestimate the total volume compared to the DFC. The magnitude of this effect can be investigated by assuming that the probability,  $p$ , of observing  $x$  particles of a given size during a single measurement followed a Poisson distribution. The Poisson cumulative distribution function is given as

$$p = F(x|\lambda) = e^{-\lambda} \sum_{x=0}^{\lambda} \frac{\lambda^x}{x!}, \quad (1)$$

where  $\lambda$  is the mean of concentration of particles, and  $x$  represents the number of particles observed in the sensing zone. For the anchor stations in Newark Bay and the Hudson River the mean number concentration of particles in size bin 32 (424–500  $\mu\text{m}$ ) was computed from the analyzed images. In Newark Bay, the number concentration was found to be  $2051 \text{ l}^{-1}$  on average, while it was  $8861 \text{ l}^{-1}$  in the Hudson River. The corresponding mean number concentrations from the Adriatic deployments were  $1671 \text{ l}^{-1}$  (Po),  $1241 \text{ l}^{-1}$  (Chienti), and  $541 \text{ l}^{-1}$  (Pescara). Assuming the particles were randomly distributed in the water column, these concentrations corresponded to an average number of particles in bin 32 in the LISST sensing zone ranging from 0.08 (Pescara) to 1.24 (Hudson River). For a single measurement, the probability that  $x = 0$ , i.e. no particles were present then varied between 0.93 (Pescara) and 0.29 (Hudson River). However, on average 30 LISST spectra

were sampled and averaged into one spectrum in Newark Bay and the Hudson River, while 50 LISST spectra were sampled and averaged into one spectrum in the Adriatic. Thus, the cumulative probability that no particles at all were present in size bin 32 in 30 or 50 measurements is  $p^{30}$  and  $p^{50}$ . This probability was less than  $2 \times 10^{-4}$  and  $6 \times 10^{-17}$  for, respectively Newark Bay and the Hudson River and less than  $9 \times 10^{-6}$ ,  $2 \times 10^{-4}$  and 0.02 for, respectively, the deployments off the Po, Chienti and Pescara Rivers. Under these conditions, the LISST should have sensed enough particles to provide an accurate estimate of mean concentration of large particles, suggesting that small particle numbers were not responsible for the disagreement between LISST and DFC volumes.

The LISST laser beam can become misaligned. Misalignment causes excessive light scattering at the innermost rings and affects the size spectrum by assigning too much volume to the largest size bins. Before and after deployment the scattering pattern of both LISSTs were checked in clean water, and compared to a factory reference scattering pattern (cf. Agrawal and Pottsmith, 2000). No discrepancies were found for either instrument. Also, misalignment would have caused the LISST to overestimate the volume concentration, which was not the case with the present data. Misalignment can thus be ruled out as an explanation for the volume difference.

The optical path length of the LISST is five cm, whereas the slab width of the DFC is 2.5 cm. When small particles are 'shadowed' by larger particles, they are not detected by either instrument, and the volume is underestimated. Conceptually, the chance that this will happen increases with increasing path length, which could have caused the LISST to underestimate the volume compared to the DFC. This effect also increases with increasing concentration. The observation that volume offset was most pronounced for the Po deployment, for which volume concentrations were lower than in Newark Bay and the Hudson River, suggests that particle overlap was not the underlying cause of volume mismatch.

Finally, also the influence of multiple scattering (re-scattering of scattered light) can be excluded as a cause of the lower volume estimates by the

LISST as the optical transmission was found to be above 30% for 99.65% of the measurements (data not shown). When the optical transmission is above 30% the influence of multiple scattering can be considered negligible (Agrawal and Pottsmith, 2000).

Merged particle size spectra (Fig. 8) were created by adjusting the LISST spectra with an appropriate coefficient and then merging them with the DFC spectra. It is important to realize that the multiplication with a correction factor had no implications for the shape of the adjusted spectrum, as it increased the volume in all size bins by the same amount. It should also be emphasized that the size range of the merged spectrum is an operational one, defined by the (arbitrary) size ranges of the LISST-100 and the DFC. Particles  $< 2.5 \mu\text{m}$  have been shown to exist in suspension (Stramski and Kiefer, 1991; Jackson et al., 1997), and are not detected by either instrument, thus they are not included in the merged spectrum. Finally, when applying the correction factor to the entire LISST spectrum it is implicitly assumed that the volume:volume relationship for particles in size bins 1–24 is similar to the volume:volume relationship for particles in size bins 25–32, from which the correction factor is obtained. At present, there is no way of knowing this, since the DFC cannot detect particles in size bins 1–24. However, there is little alternative to making this assumption.

An often used operational definition for suspended matter is that which is retained on a  $0.45 \mu\text{m}$  filter after filtration (Eisma, 1993). By combining the LISST and DFC spectra it is possible to detect all suspended particles  $> 2.5 \mu\text{m}$ , so most suspended particle volume can now be detected in situ. Of all the parameters used to describe the state of flocculated, suspended matter the floc fraction—the weight % of the suspended matter that is flocculated—is the most difficult to measure. Several approaches exist for estimating the floc fraction (Fox et al., 2004b), but they rely on various assumptions: One method uses the Mikkelsen/Pejrup method (Mikkelsen and Pejrup, 2000, 2001), whereby floc density is computed from knowledge of total floc volume and mass, the latter obtained from filtered water samples or calibrated transmissometers. Using

Stokes' Law, the bulk settling velocity can then be computed as a function of floc size and compared to a measured size-settling velocity relationship (Fox et al., 2004b). The Mikkelsen/Pejrup approach implicitly assumes a floc fraction of 1, so the offset between the two size-settling velocity relationships can be used to compute floc fraction (Fox et al., 2004b). Another method employs Stokes' Law to estimate floc density, hence mass, from settling flocs captured on video tape (Fox et al., 2004b). However, the applicability of Stokes' Law for floc studies has in recent years been questioned (Li and Logan, 1997). This is presumably due to the fact that flocs are porous and permeable, which changes the drag on the floc as fluid is channelled through the pores (Li and Logan, 1997). Yet another method uses grain-size parameterization of the bed sediment (Kranck et al., 1996) in conjunction with an assumption of a constant floc settling velocity for all flocs to derive the floc fraction (Fox et al., 2004b).

If knowledge of the mass of suspended matter across the entire particle size spectrum can be obtained it is possible to estimate floc fraction simply by defining a 'cut-off' particle size, where all particles less than this size are assumed to exist as single grains, and all particles larger than this size are assumed to exist as flocs. In order to obtain the in situ mass distribution it is necessary to convert the particle volume in the individual size bins into mass by applying an appropriate size-density relationship. Khelifa and Hill (accepted) suggested the following model for obtaining effective floc density as a function of floc size, fractal dimension and the size of the single grains making up the floc:

$$\rho_f - \rho_w = \rho_s - \rho_w \left( \frac{D_f}{d_{50}} \right)^{F-3} \varphi, \quad (2)$$

where  $\rho_f$  is the floc density,  $\rho_w$  is the density of the water,  $\rho_s$  is the density of the single grains making up the floc,  $D_f$  is floc diameter,  $d_{50}$  is the median diameter of the single grains making up the floc,  $F$  is the fractal dimension of the floc described by a function that allows  $F$  to decrease as floc size increases, and  $\varphi$  has a value of 1 (for details, see Khelifa and Hill, accepted). Using Eq. (2) and

values for  $\rho_s$ ,  $d_{50}$ , and  $\varphi$  as recommended by Khelifa and Hill (accepted) the volume of the particles in each size bin for all spectra in Fig. 8 was converted to mass, and the floc fraction was computed for four diameters representing the 'cut-off' particle size: 8, 16, 32 and 64  $\mu\text{m}$  (Table 6). The floc fraction is independent of which spectrum is adjusted (the LISST spectrum to the DFC spectrum or vice versa). This is because the floc fraction computed from a given spectrum is not related to the actual volume concentration in the bins of the spectrum, but only to the relative difference in volume between the bins. The cut-off size is thought to represent the division between single grains and flocs, i.e. all particles smaller than the cut-off size are thought to exist as single grains whereas all flocs larger than the cut-off size are thought to exist as flocs. The four sizes chosen yield an opportunity to estimate the sensitivity of the choice of the cut-off size on the computed floc fraction.

Depending on the cut-off size, floc fraction for the 15 spectra varied between 0.34 and 0.95 (Table 6), in agreement with previous studies (Syvitski et al., 1995; Fox et al., 2004b). It is seen that the trend of changes in floc fraction between

Table 6  
Floc fractions for the spectra in Fig. 8, computed for four different cut-off diameters

Spectrum	Floc fraction for a cut-off diameter of			
	8 $\mu\text{m}$	16 $\mu\text{m}$	32 $\mu\text{m}$	64 $\mu\text{m}$
A	0.95	0.91	0.89	0.88
B	0.76	0.60	0.47	0.35
C	0.66	0.51	0.40	0.30
D	0.92	0.90	0.88	0.87
E	0.88	0.85	0.82	0.78
F	0.72	0.66	0.62	0.57
G	0.76	0.67	0.58	0.49
H	0.66	0.55	0.46	0.36
I	0.73	0.63	0.54	0.44
J	0.90	0.83	0.75	0.67
K	0.85	0.75	0.65	0.59
L	0.90	0.83	0.73	0.62
M	0.80	0.67	0.47	0.34
N	0.82	0.72	0.58	0.40
O	0.86	0.76	0.64	0.50

different spectra is the same for all cut-off diameters while the absolute values obviously changes, i.e. as the cut-off diameter increases the flocs fraction decreases. These results demonstrate that the merged size spectra in conjunction with a consistent way of converting the volume distribution to mass enable determination of floc fraction. Future studies could benefit by focusing effort on determining what an appropriate cut-off diameter would be, as well as by simultaneously measuring the suspended matter concentration from water samples. With these data it would be possible to evaluate how well the model of [Khelifa and Hill \(accepted\)](#) converts volume to mass, as well as deducing which of the two instruments is the more accurate in estimating volume concentration.

The merged spectra generally revealed size distributions that differ from spectra typically assumed by models of water column optical properties. Such models assume that particle size follows the Junge distribution, for which volume is approximately constant in logarithmically increasing size bins ([Boss et al., 2001](#); [Stramski et al., 2001](#)). Merged spectra typically had equal volumes in size classes smaller than approximately 100  $\mu\text{m}$ , but they tended to be peaked at larger sizes. These spectra are consistent with the hypothesis that suspensions comprise flocs and single grains, with flocs accounting for most of the suspended mass and the peak in the grain size distribution and single grains accounting for the fine, flat tail of the distribution (e.g. [Curran et al., 2002, 2004](#); [Fox et al., 2004a](#)). They are also consistent with recent evidence that flocs are more important to the optical properties of the water column than previously believed ([Hatcher et al., 2001](#); [Mikkelsen, 2002b](#); [Flory et al., 2004](#)).

While this work demonstrates the feasibility of merging size spectra from the two different instruments it would be more desirable to measure the entire size distribution with a single instrument. At present, an extended version of the LISST, the LISST-FLOC, covers the size range 7.5–1500  $\mu\text{m}$ , probably making it suitable for most flocculation studies. However, since its lower limit has been increased, its usefulness for marine optics studies may be lessened. Large flocs are highly porous, and the scattering characteristics of such

porous aggregates are by and large unknown. Hence it would be desirable to compare results obtained with the LISST-FLOC with results from a DFC. This could confirm the ability of laser particle sizers to measure the size and volume of highly porous structures, and could potentially also lead to new insight of the scattering properties of such porous aggregates.

## 5. Conclusions

In situ particle size and volume concentration ( $VC$ ) data were obtained during five simultaneous deployments of a LISST-100 in situ laser diffraction particle sizer and a digital floc camera in Newark Bay, the Hudson River and the Adriatic Sea. The two instruments overlapped in the size range 135–500  $\mu\text{m}$ .

In the Adriatic,  $D_{50}$  from the two instruments showed the same temporal variation; however,  $D_{50}$  from the DFC was consistently higher than  $D_{50}$  from the LISST by a factor of 2–3. Trimming the size spectra from both instruments, so that the particle diameter was computed using only the overlapping bins (25–32) removed this offset.

In Newark Bay and the Hudson River, LISST  $D_{50}$  was higher than DFC  $D_{50}$  by a factor of approximately 2. This offset was due to the influence of particles  $>500 \mu\text{m}$ , which caused excessive light scattering on LISST detector rings 31–32. Trimming the size spectra from both instruments, so that the particle diameter was computed using only the overlapping bins without excessive light scattering (bins 25–30), removed this offset.

The  $VC$  in the overlapping size bins were compared for the two instruments. The LISST generally provided a lower estimate of  $VC$  than the DFC. The offset in volume between the two instruments was approximately a factor of 3. Numerous reasons for the volume underestimation were explored. One reason could be potential variation in the LISST volume conversion coefficient across the size bins, while another could be the thresholding value used when analyzing digital images. The fact that the two instruments did not

detect the same volume in the overlapping size bins was surprising and is an issue that deserves more attention. Accurate measurements of in situ *VC* are essential for flocculation and sedimentation studies as well as for marine optics studies.

A method was presented for matching the *VC* from the two instruments in the region of overlap. This method largely eliminated the offset and made it possible to combine the spectra from the LISST with the spectra from the DFC, thereby creating merged in situ particle size spectra with a dynamic range of roughly 1:4000, covering sizes from 2.5 to 9900  $\mu\text{m}$ . The particle volume across the merged size spectra was converted to mass, enabling estimates of floc fraction. Floc fraction values fell between 0.34 and 0.95, which is within that reported by other workers. Future flocculation studies could benefit from obtaining merged size spectra together with measurement of the concentration of suspended particulate matter. This could be used to determine which of the two instruments is the more accurate in estimating volume.

### Acknowledgements

The fieldwork in the Adriatic Sea was carried out as part of the EuroSTRATAFORM program, funded by grants #N00014-97-1-0160, N00014-99-1-0113, and N00014-04-1-0165, N00014-04-1-0182, from the Office of Naval Research (USA). O.A.M. was supported by postdoctoral fellowship grants #21-01-0435, 21-02-0292 from the Danish Natural Science Research Council. The fieldwork in the Newark Bay area was funded by New York Port Authority and the New Jersey Department of Transportation. The crew of 'RV Seward Johnson II' is thanked for their help during the fieldwork in the Adriatic Sea. Brent Law and Andrew Stewart are thanked for helping out with the fieldwork. Peter Traykovski from Woods Hole Oceanographic Institution lent us the LISST-100 used for the Adriatic field work. The comments and suggestions from several anonymous reviewers were highly appreciated and substantially improved crucial parts of the manuscript.

### References

- Agrawal, Y.C., Pottsmith, H.C., 2000. Instruments for particle size and settling velocity observations in sediment transport. *Marine Geology* 168, 89–114.
- Bale, A.J., Morris, A.W., 1987. In situ measurement of particle size in estuarine waters. *Estuarine, Coastal and Shelf Science* 24, 253–263.
- Boss, E., Pegau, W.S., Gardner, W.D., Zaneveld, J.R.V., Barnard, A.H., Twardowski, M.S., Chang, G.C., Dickey, T.D., 2001. Spectral particulate attenuation and particle size distribution in the bottom boundary layer of a continental shelf. *Journal of Geophysical Research* 106, 9509–9516.
- Chen, S., Eisma, D., 1995. Fractal geometry of in situ flocs in the estuarine and coastal environments. *Netherlands Journal of Sea Research* 32, 173–182.
- Curran, K.J., Hill, P.S., Milligan, T.G., 2002. The role of particle aggregation in size-dependent deposition of drill mud. *Continental Shelf Research* 22, 405–416.
- Curran, K.J., Hill, P.S., Schell, T.M., Milligan, T.G., Piper, D.J.W., 2004. Inferring the mass fraction of floc-deposited mud: application to fine-grained turbidites. *Sedimentology* 51, 927–944.
- Eisma, D., 1993. *Suspended Matter in the Aquatic Environment*. Springer, Berlin.
- Eisma, D., Schuhmacher, T., Boekel, H., van Heerwaarden, J., Franken, H., Laan, M., Vaars, A., Eijgenraam, F., Kalf, J., 1990. A camera and image-analysis system for in situ observation of flocs in natural waters. *Netherlands Journal of Sea Research* 27, 43–56.
- Flory, E.N., Hill, P.S., Milligan, T.G., Grant, J., 2004. The relationship between floc area and backscatter during a spring phytoplankton bloom. *Deep-Sea Research I* 51, 213–223.
- Fox, J.M., Hill, P.S., Milligan, T.G., Boldrin, A., 2004a. Flocculation and sedimentation on the Po River delta. *Marine Geology* 203, 95–107.
- Fox, J.M., Hill, P.S., Milligan, T.G., Ogston, A.S., Boldrin, A., 2004b. Floc fraction in the waters of the Po River prodelta. *Continental Shelf Research* 24, 1699–1715.
- Gartner, J.W., Cheng, R.T., Wang, P.-F., Richter, K., 2001. Laboratory and field evaluations of the LISST-100 instrument for suspended particle size determinations. *Marine Geology* 175, 199–219.
- Geyer, W.R., Woodruff, J.D., Traykovski, P., 2001. Sediment transport and trapping in the Hudson River estuary. *Estuaries* 24, 670–679.
- Grosjean, P., Picheral, M., Warembourg, C., Gorsky, G., 2004. Enumeration, measurement, and identification of net zooplankton samples using the ZOOSCAN digital imaging system. *ICES Journal of Marine Science* 61, 518–525.
- Hatcher, A., Hill, P.S., Grant, J., 2001. Optical backscatter of marine flocs. *Journal of Sea Research* 46, 1–12.
- Hill, P.S., Syvitski, J.P.M., Cowan, E.A., Powell, R.D., 1998. In situ observations of floc settling velocities in Glacier Bay, Alaska. *Marine Geology* 145, 85–94.

- Hill, P.S., Voulgaris, G., Trowbridge, J.H., 2001. Controls on floc size in a continental shelf bottom boundary layer. *Journal of Geophysical Research* 106, 9543–9549.
- Jackson, G.A., Maffione, R., Costello, D.K., Alldredge, A.L., Logan, B.E., Dam, H.G., 1997. Particle size spectra between 1  $\mu$ m and 1 cm at Monterey Bay determined using multiple instruments. *Deep-Sea Research I* 44, 1739–1767.
- Khelifa, A., Hill, P.S., accepted. Models for effective density and settling velocity of flocs. *Journal of Hydraulic Research*.
- Knowles, S.C., Wells, J.T., 1996. Suspended aggregate analysis using ISAAC, Elbe river, 9–10 June 1993. *Journal of Sea Research* 36, 69–75.
- Kranck, K., Smith, P.C., Milligan, T.G., 1996. Grain size characteristics of fine grained unflocculated sediments I: “one-round” distributions. *Sedimentology* 43, 589–596.
- Law, D.J., Bale, A.J., Jones, S.E., 1997. Adaptation of focused beam reflectance measurement to in-situ particle sizing in estuaries and coastal waters. *Marine Geology* 140, 47–59.
- Li, X., Logan, B.E., 1997. Collision frequencies of fractal aggregates with small particles by differential settling. *Environmental Science and Technology* 31, 1229–1236.
- Maldiney, M.-A., Mouchel, J.-M., 1996. In situ video recording of suspended flocs. *Journal of Sea Research* 36, 87–91.
- Mikkelsen, O.A., 2002a. Variation in the projected surface area of suspended particles: Implications for remote sensing assessment of TSM. *Remote Sensing of Environment* 79, 23–29.
- Mikkelsen, O.A., 2002b. Examples of spatial and temporal variations of some fine-grained suspended particle characteristics in two Danish coastal water bodies. *Oceanologica Acta* 25, 39–49.
- Mikkelsen, O.A., Pejrup, M., 2000. In situ particle size spectra and density of particle aggregates in a dredging plume. *Marine Geology* 170, 443–459.
- Mikkelsen, O.A., Pejrup, M., 2001. The use of a LISST-100 laser particle sizer for in-situ estimates of floc size, density and settling velocity. *Geo-Marine Letters* 20, 187–195.
- Mikkelsen, O.A., Milligan, T.G., Hill, P.S., Moffatt, D., 2004. INSSECT—an instrumented platform for investigating floc properties close to the seabed. *Limnology & Oceanography: Methods* 2, 226–236.
- Milligan, T.G., 1996. In situ particle (floc) size measurements with the Benthos 373 plankton silhouette camera. *Journal of Sea Research* 36, 93–100.
- Otsu, N., 1979. A threshold selection method from gray-level histograms. *IEEE Transactions on Systems, Man, and Cybernetics* 9, 62–66.
- Stramski, D., Kiefer, D.A., 1991. Light scattering by microorganisms in the Open Ocean. *Progress in Oceanography* 28, 343–383.
- Stramski, D., Bricaud, A., Morel, A., 2001. Modeling the inherent optical properties of the ocean based on the detailed composition of the planktonic community. *Applied Optics* 40, 2929–2945.
- Syvitski, J.P.M., Hutton, E.W.H., 1996. In situ characteristics of suspended particles as determined by the floc camera assembly FCA. *Journal of Sea Research* 36, 131–142.
- Syvitski, J.P.M., Asprey, K.W., Leblanc, K.W.G., 1995. In-situ characteristics of particles settling within a deep-water estuary. *Deep-Sea Research II* 42, 223–256.
- Thomsen, L., Jähmlich, S., Graf, G., Friedrichs, M., Springer, B., Wanner, B., 1996. An instrument for aggregate studies in the benthic boundary layer. *Marine Geology* 135, 153–157.
- Traykovski, P., Latter, R.J., Irish, J.D., 1999. A laboratory evaluation of the laser in situ scattering and transmissometry instrument using natural sediments. *Marine Geology* 159, 355–367.
- Ulloa, O., Sathyendranath, S., Platt, T., 1994. Effect of the particle-size distribution on the backscattering ratio in seawater. *Applied Optics* 33, 7070–7077.
- Van der Lee, W.T.B., 1998. The impact of fluid shear and the suspended sediment concentration on the mud floc size variation in the Dollard estuary, The Netherlands. In: Black, K.S., Patterson, D.M., Cramp, A. (Eds.), *Sedimentary Processes in the Intertidal Zone*, vol. 139. Geological Society, London, UK, pp. 187–198.
- Van Leussen, W., 1994. Estuarine macroflocs and their role in fine-grained sediment transport. Ph.D. Thesis, Utrecht University, The Netherlands, unpublished.
- Van Leussen, W., Cornelisse, J.M., 1996. The underwater video system VIS. *Journal of Sea Research* 36, 77–81.